Porphyrin Based Self-Assembled Monolayer Thin Films: Synthesis and Characterization

DeQuan Li,* Basil I. Swanson, Jeanne M. Robinson, and Mark A. Hoffbauer

Contribution from the Isotope and Nuclear Chemistry Division and the Chemical and Laser Sciences Division, Los Alamos National Laboratory, Los Alamos, New Mexico 87545

Received February 5, 1993

Abstract: The synthesis and characterization of covalently bound self-assembled monolayer thin films of 5,10,15,20-tetra(4-pyridyl)-21*H*,23*H*-porphine (TPyP) and its derivatives on fused quartz and silicon ⟨100⟩ substrates having a native oxide layer are described. The monolayer film consists of porphyrin macrocycle disk-like structures that were analyzed by UV–visible spectroscopy, X-ray photoelectron spectroscopy (XPS), and polarized FTIR-ATR measurements. One of the attractive features of these complexes is their large second-order nonlinear optical response, as expected for a strongly delocalized π-electron system without inversion symmetry. Second-harmonic generation (SHG) measurements have been used to determine the absolute value of the dominant element of the nonlinear susceptibility, $\chi_{zzz} \sim 2 \times 10^{-8}$ esu, the uniformity of these films, and the dispersion of the refractive indices. The average molecular orientation angle of the surface-bound chromophores was measured by both FTIR-ATR and SHG and found to be in good agreement.

Introduction

Molecular architecture and molecular engineering of artificial, supermolecular, self-assemblies at surfaces (or interfaces) with desired structures and physical properties have attracted great interest recently.[1] Monolayer[2] and multilayer[3] formation, such as alkylsilanes on glass or alkanethiols on gold, offer a potential starting point for fabricating highly ordered multifunctional thin films. The central advantage of using covalently bound self-assembly schemes is that the weak van der Waals interactions or hydrogen bonding between interfaces, as in the case of Langmuir–Blodgett films, are replaced with covalent bonds. Moreover, uniform film thickness and dense coverage can be achieved by properly choosing the reagent which will be anchored on the well-defined surface functional groups. Excess deposition can also be eliminated because the surface reaction stops as soon as the surface functional groups are consumed.

Highly ordered, molecular solid assemblies can lead to materials with extremely interesting properties such as a high nonlinear optical (NLO) susceptibility,[4] isotropic conduction,[5] and permanent magnetism,[6] but their syntheses[7] are extremely challenging. Studies of these assemblies have been motivated by their relevance to a variety of solid-state phenomena including nonlinear optics, electrochemistry, and monolayer catalysis. Classical Langmuir–Blodgett monolayers and polymeric thin films represent encouraging approaches to nonlinear optical materials and their potential applications. Nonetheless, long-term stability, poor adhesion to substrates, uniformity, and polymer swelling are significant issues in the use of these materials. We report here the synthesis and optical characterization of molecular assemblies consisting of a disk-like macrocycle complex based on covalent binding of 5,10,15,20-tetra(4-pyridyl)-21*H*,23*H*-porphine (TPyP) monolayer to the surface silicon oxide.

The central focus of construction of supermolecular architecture is incorporating built-in multifunctionalities such as multidentate ligands, (non)linear optical properties, or catalytic properties into complex, multimolecule superstructures. The present molecular building block, TPyP, offers multidentate pyridyl ligands with highly delocalized π-electrons which yield the desired nonlinear optical properties when the pyridyl group on the porphyrin is quaternized to form a noncentrosymmetric structure. The growth of the porphyrin molecular self-assemblies can be easily monitored by the distinctive porphyrin Soret band. Compared to the traditional molecular self-assemblies of straight-chain alkanes, the present disk-like porphyrin molecular self-assemblies are more interesting and also more challenging. Complex supermolecular self-assemblies which can be built from either inorganic complexes or organic materials are of potential technological use in catalysis, microelectronics, and optics.

Experimental Section

All synthetic procedures described below were carried out under an argon atmosphere. The fused quartz substrates were ultrasonically cleaned in 10% detergent solution for 10 min and then refluxed in 1% tetrasodium ethylenediamine tetraacetate (EDTA) solution for 10 min, followed by another 10-min sonication at ambient temperature. Finally, the substrates were thoroughly rinsed with deionized water and acetone and then sputter cleaned using an argon plasma at 0.5 Torr for >30 min. Polished Si wafers were cleaned by sonicating in 10% detergent solution for 10 min and then sputter cleaned using an argon plasma for 30 min. All substrates were used immediately after cleaning.

Formation of the self-assembled porphyrin monolayers consisted of two primary steps: (1) coupling layer formation and (2) porphyrin layer

(1) (a) Lee, H.; Kepley, L. J.; Hong, H. G.; Mallouk, T. E. *J. Am. Chem. Soc.* **1988**, *110*, 618–620. (b) Ulman, A.; Tillman, N. *Langmuir* **1989**, *5*, 1418–1420. (c) Pomerantz, M.; Segmuller, A.; Netzer, L.; Sagiv, J. *Thin Solid Films* **1985**, *132*, 153–162. (d) Putvinski, T. M.; Schilling, M. L.; Katz, H. E.; Chidsey, C. E. D.; Mujsce, A. M.; Emerson, A. B. *Langmuir* **1990**, *6*, 1567–1571. (e) Allara, D. L.; Atre, S. V.; Elliger, C. A.; Snyder, R. G. *J. Am. Chem. Soc.* **1991**, *113*, 1852–1854.

(2) Wasserman, S. R.; Tao, Y. T.; Whitesides, G. M. *Langmuir* **1989**, *5*, 1074–1087.

(3) Maoz, R.; Sagiv, J. *J. Colloid Interface Sci.* **1984**, *100* (2), 465–496.

(4) (a) Li, D.; Ratner, M. A.; Marks, T. J.; Zhang, C.; Yang, J.; Wang, G. K. *J. Am. Chem. Soc.* **1990**, *112*, 7389–90. (b) Li, D.; Marks, T. J.; Zhang, C.; Yang, J.; Wang, G. K. *Proc. SPIE—Int. Soc. Opt. Eng.* **1990**, *1337*, 341–7. (c) Li, D.; Marks, T. J.; Zhang, C.; Wang, G. K. *Synth. Met.* **1991**, *41–43*, 3157–62. (d) Katz, H. E.; Scheller, G.; Putvinski, T. M.; Schilling, M. L.; Wilson, W. L.; Chidsey, C. E. D. *Science* **1991**, *254*, 1485–7.

(5) (a) Ueda, N.; Kawazoe, H.; Watanabe, Y.; Takata, M.; Yamane, M.; Kubodera, K. *Appl. Phys. Lett.* **1991**, *59* (5), 502–3. (b) Kato, H.; Nishikawa, O.; Matsui, T.; Honma, S.; Kokado, H. *J. Phys. Chem.* **1991**, *95* (15), 6014–6.

(6) (a) Aldrovandi, S.; Borsa, F.; Lascialfari, A.; Tongnetti, V. *J. Appl. Phys.* **1990**, *67* (9, 2A), 5052–4. (b) Levy, P. M.; Ounadjela, K.; Wang, Y.; Sommers, C. B.; Fert, A. *J. Appl. Phys.* **1990**, *67* (9, 2B), 5914–19.

(7) (a) Schildkraut, J. S.; Penner, T. L.; Willand, C. S.; Ulman, A. *Opt. Lett.* **1988**, *13*, 134–6. (b) Lupo, D.; Prass, W.; Schunemann, U.; Laschewsky, A.; Ringsdorf, H.; Ledoux, I. *J. Opt. Soc. Am. B* **1988**, *5*, 300–8. (c) Ledoux, I.; Josse, D.; Vidakovic, P.; Zyss, J.; Hann, R. A.; Gordon, P. F.; Bothwell, B. D.; Gupta, S. K.; Allen, S.; Robin, P.; Chastaing, E.; Dubois, J. C. *Europhys. Lett.* **1987**, *3*, 803–9. (d) Hayden, L. M.; Kowel, S. T.; Srinivasan, M. P. *Opt. Commun.* **1987**, *61*, 351–6.

0002-7863/93/1515-6975$04.00/0

addition. The porphyrin layer was either quaternized or protonated in subsequent steps (3a, 3b).

1. Coupling Layer (Cp) Formation. The clean substrates were immersed in a dry $CHCl_3$ solution containing either 0.13 M (*p*-(chloromethyl)phenyl)trichlorosilane or (*p*-(iodomethyl)phenyl)triiodosilane at room temperature for 24 h. The substrates were transferred into a neat $CHCl_3$ solution and cleaned by 2-min sonication. This procedure was repeated four times. The silane-coated substrates were rinsed with acetone and dried in air.

The following data characterize the formation of the coupling layer (Cp layer: $Cl_3SiC_6H_4CH_2X + SiO_2$, where X = Cl or I). Advancing contact angle: quartz, $\theta_a(H_2O) = 5°$; Cp, $\theta_a(H_2O) = 50°$. UV–vis spectrum (monolayer of Cp on quartz): $\lambda_{max} = 195$ nm ($A = 0.241$). FTIR-ATR (monolayer of Cp on Si wafer): $\nu_{16} + \nu_5 = 1605\ cm^{-1}$ (phenyl ring vib), $\nu_1 + \nu_6 = 1396\ cm^{-1}$ (phenyl ring vib).

2. Porphyrin Layer (TPyP) Addition. A monolayer of the TPyP was covalently attached to the coupling layer Cp by refluxing the substrates coated with coupling layers in an ethanol/chloroform (1:9) solution of 1.5 mM TPyP for 2 days at 90–100 °C. The porphyrin-coated substrates were transferred into a mixed solvent of EtOH and $CHCl_3$ (1:9 by volume) and then cleaned by repeated sonication as described above. After cleaning, the substrates were thoroughly rinsed with acetone and dried in air.

The following data characterize the porphyrin layer formation. UV–vis spectrum (monolayer of CpTPyP on quartz): $\lambda_{max} = 447$ nm ($A = 0.0259$). Elements identified by XPS: C(1s), N(1s), O(1s), Si(2s and 2p), and Cl(2p) or I(3d). FTIR-ATR (monolayer of CpTPyP on Si wafer): $\nu(C_\alpha–C_m) = 1724\ cm^{-1}$ (br), $\nu_{8a} = 1635\ cm^{-1}$ (pyridinium group), $\nu_4 = 1593\ cm^{-1}$ (pyridyl group), $\nu(C_\beta–C_m) + \delta(CCN) = 1450\ cm^{-1}$, $\nu = 1404\ cm^{-1}$ (phenyl group).

3a. Quaternization of Porphyrin Layer (TMPyP). The CpTPyP derivatized monolayer was then refluxed in the same mixed solvent solution containing 3.2 M iodomethane at 90–110 °C (oil bath temperature) for 2 days. The substrates were then cleaned by repeated rinsing and sonication in the mixed EtOH/$CHCl_3$ solvent.

The following data characterize the quaternization of the porphyrin layer. UV–vis spectrum (monolayer of CpTMPyP on quartz): $\lambda_{max} = 437$ nm ($A = 0.0262$). XPS: C(1s), N(1s), O(1s), Si(2s and 2p), and Cl(2p) or I(3d). FTIR-ATR (monolayer of CpTMPyP on Si wafer): $\nu(C_\alpha–C_m) = 1724\ cm^{-1}$ (br), $\nu_{8a} = 1635\ cm^{-1}$ (pyridinium group), $\nu = 1605\ cm^{-1}$ (phenyl group), $\nu(C_\beta–C_m) + \delta(CCN) = 1458\ cm^{-1}$, $\nu = 1400\ cm^{-1}$ (phenyl group).

Quaternizations of the CpTPyP monolayer with benzyl chloride or allyl chloride were carried out in a similar manner. Reaction conditions: $[C_6H_5CH_2Cl] = 0.10$ M; $[CH_2CHCH_2Cl] = 0.40$ M; solvent, $CHCl_3$/EtOH, 9:1 by volume; temperature, 90–110 °C.

3b. Protonation of Porphyrin Layer (THPyP). The CpTPyP monolayer coated substrates were immersed in a concentrated HCl (37%) aqueous solution for 5 min. The substrates were withdrawn from the solution and sonicated four times in deionized water with a 2-min duration period for each sonication. The protonated porphyrin layer was then rinsed with deionized water and acetone and dried in air. UV–vis spectrum (monolayer of CpTHPyP on quartz): $\lambda_{max} = 437$ nm.

FTIR-ATR Measurement. The infrared spectra of porphyrin monolayer thin films were collected using a Bio-Rad FTS-40 with a Harrick Seagull variable-angle reflection attachment. The porphyrin monolayer was studied using the internal attenuated total reflection (ATR) mode in which the Si wafer functionalized with an organic monolayer was pressed against a ZnSe hemisphere crystal with a miniature pressure device to assure optical contact. A single attenuated total reflection from the interface of the ZnSe hemisphere crystal and the Si wafer was collected with 1024 scans and 8 cm^{-1} resolution. This approach allows the angle of incidence to be varied from 5° to 85°. The critical incident angle, $\theta_c = 39°$, used in this work yields the maximum signal because strong interaction of the infrared radiation with the interface of the ZnSe hemisphere crystal and the Si wafer occurs at this geometry.

SHG Measurement. The nonlinear optical properties of the monolayer films were investigated using second-harmonic generation (SHG) in a transmission geometry. The SHG measurements were made using the 1064-nm light from a 30-Hz Nd:YAG regenerative amplifier system that provided ~100-ps pulses with energies at the thin-film surface of 200–400 μJ. The p- or s-polarized incident laser was mildly focused onto the surface (spot size ~1 mm in diameter). The transmitted SHG signal at 532 nm was separated from the fundamental beam using a dichroic mirror and color filters, passed through a polarization analyzer to select either the p- or s-polarized component, and detected using a cooled photomultiplier tube. A gated boxcar integrator was used to measure the transmitted second-harmonic signal as the substrate was rotated from normal incidence (0°) to grazing incidence (~90°).

Scheme I

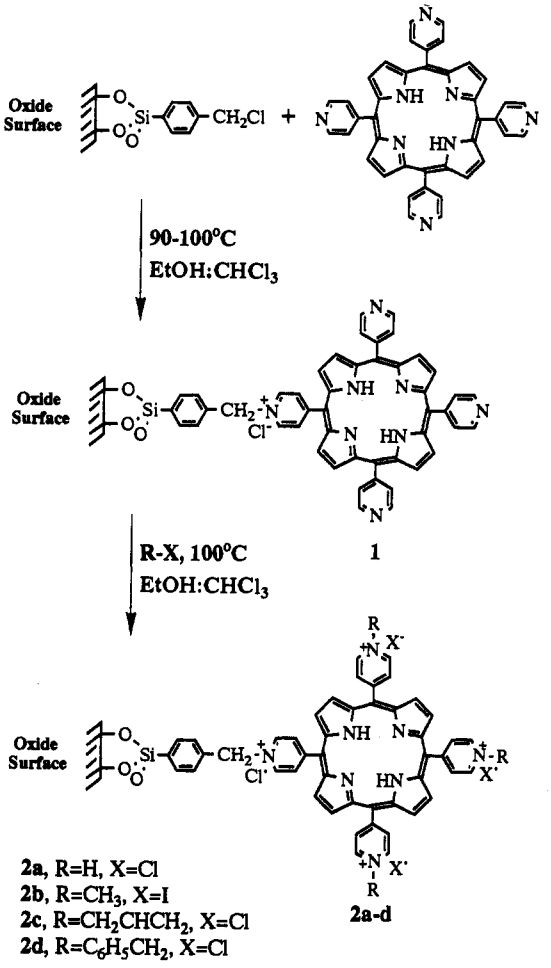

Results and Discussion

Preparation of Covalently Bound Self-Assembled Porphyrin Monolayers. The general strategy we have employed for synthesizing the self-assembled monolayers is summarized in Scheme I.[4] The silane–based coupling layer (Cp) is bound to the surface oxide (SiO_2) via a siloxane linkage[8] that provides chemical and structural stability in addition to structural regularity, as controlled by the density of surface hydroxyl groups,[9] i.e., approximately one hydroxyl group per 20 Å^2. After anchoring the porphyrin macrocycle to form the self-assembled CpTPyP monolayer, a characteristic change in its electronic spectrum[10] along with its signature in X-ray photoelectron spectroscopy (XPS)[11] was observed, suggesting the quaternization of the pyridyl group. The attenuation of the substrate signals (Si and O) by the porphyrin thin films corresponds to a monolayer-thick overlayer on the fused silica substrates. The simultaneous appearance of both pyridyl groups and pyridinium groups in the infrared spectra confirms the quaternization of the pyridyl group on the porphyrin, i.e., an acentric porphyrin structure. The CpTPyP film was subsequently either quaternized or protonated.

(8) Cp layer: $Cl_3SiC_6H_4CH_2X + SiO_2$, where X = Cl or I. Advancing contact angle: quartz, $\theta_a(H_2O) = 5°$; Cp, $\theta_a(H_2O) = 50°$. UV–vis: $\lambda_{max} = 195$ nm.

(9) Wasserman, S. R.; Whitesides, G. M.; Tidswell, I. M.; Ocko, B. M.; Pershan, P. S.; Axe, J. D. *J. Am. Chem. Soc.* **1989**, *111*, 5852–61.

(10) $\lambda_{max} = 447$ nm (porphyrin-based monolayer) vs 412 nm for 5,10,15,20-tetra(4-pyridyl)-21*H*,23*H*-porphine.

(11) XPS: C(1s), N(1s), O(1s), Si(2s and 2p), and Cl(2p) or I(3d).

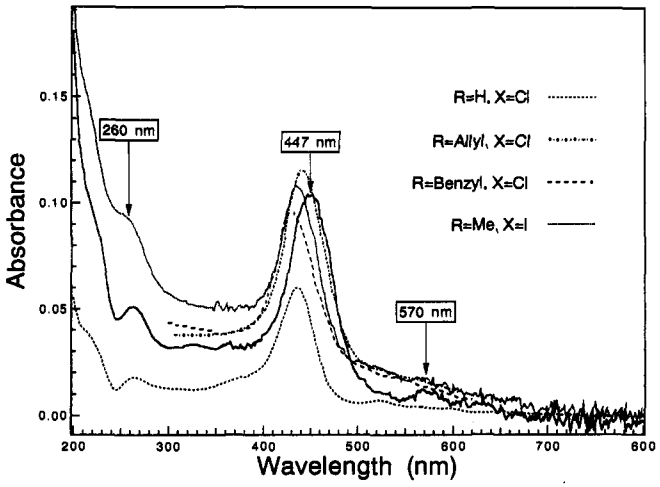

Figure 1. Optical absorption before (CpTPyP) and after ($CpTRPyP^+X^-$) reacting monolayer CpTPyP with various analytes. The spectra are collected from four individual monolayer thin films on both sides of two substrates. Therefore, each individual monolayer has only a quarter of the intensity shown in this graph.

Scheme I illustrates the quaternization of the aromatic porphyrin ring upon reaction of various analytes and, in particular, with halogenated hydrocarbons. For example, the porphyrin monolayer can be fully quaternized by reacting this CpTPyP monolayer with iodomethane. The completion of the quaternization reaction is indicated by the complete disappearance of the pyridyl group vibrational mode in the infrared spectra and the corresponding increase in the pyridinium vibrational group mode. Similarly, the available pyridyl groups can also be protonated by immersing the CpTPyP film in an aqueous solution of concentrated hydrochloride acid (37%) for a short period of time. The protonation reaction is confirmed by the optical absorption shifts of the porphyrin Soret band and the α-band.

Electronic Optical Absorption. The observed optical absorption spectrum shown in Figure 1 indicates that the π electrons are highly delocalized, with the strong porphyrin Soret band at $\lambda_{max} \sim 447$ nm and the weak α-band at 570 nm. Using the Beer–Lambert law $A = \epsilon lc$, where A is the absorbance and ϵ, l, and c are the extinction coefficient, the thickness of film, and the concentration of porphyrin within the film, respectively, one can calculate the surface coverage, $d_{surf} = A\epsilon^{-1}$. Using the extinction coefficient of the model compound 5,10,15,20-tetrakis(1-methyl-4-pyridyl)-21*H*,23*H*-porphine tetra-p-tosylate salt ($\lambda_{max}(H_2O) = 422$ nm; $\epsilon = 1.5 \times 10^5\ cm^{-1}\ M^{-1}$), the estimated surface density[12] of the porphyrin macrocycle is $\sim 2 \times 10^{-7}$ mmol/cm^2 or ~ 1.2 porphyrin macrocycle per 100 Å^2. By employing the estimated thickness of ~ 17 Å (*vide infra*) and this surface coverage, a molecular packing density of 1 porphyrin per 1.04 nm^3 was obtained. The crystallography packing density[13] of TPyP is 1 molecule per 0.99 nm^3. Thus, the present covalently bound self-assembled porphyrin monolayers are densely packed. The absorbance intensity of the Soret band remains relatively constant before and after the quaternization. The half-width of the absorption peak is about 50 nm for the covalently bound thin films in contrast to 15 nm for the dilute solution of TPyP in chloroform. The broadening of the absorption spectra arises from intermolecular close packing and the cofacial, intermolecular π-electron interactions in condensed solid-state thin films, which is consistent with a dense monolayer coverage.

Upon exposure of CpTPyP to iodomethane, a distinct 10-nm blue shift of the major feature Soret band in the UV–vis spectrum (Figure 1) concomitant with the quaternization of available pyridyl groups on the porphyrin skeleton occurs, i.e., the formation of assembly **2**, $CpTRPyP^+X^-$, where R = CH_3 and X = I^- (Scheme I). The optical shift to the blue is due to the destruction of the acentric structure in assembly **1** together with its intramolecular charge transfer[14] and the formation of centrosymmetric porphyrin assemblies **2a–d**. The 260-nm absorption feature remains largely unchanged during the quaternization. No detectable changes were observed in the UV–visible absorption spectra for films stored in air at ambient temperatures for 1 month. Protonation of the available pyridyl groups on the porphyrin skeleton in aqueous solution also induces a diagnostic 10-nm blue shift. In addition to the shift of the porphyrin Soret band, the α-band shift from 570 to 540 nm was also visible, as illustrated in Figure 1. The 260-nm absorption feature was not significantly affected by the protonation.

Polarized Internal Attenuated Total Reflection Infrared Spectroscopy. Internal attenuated total reflection infrared spectroscopy (FTIR-ATR) was used to characterize the monolayer thin films. Traditional techniques for monolayer materials involve either reflection at fixed grazing incidence angles, typically from metallic surfaces, or waveguiding multireflection using expensive optical prisms whose surfaces are modified by chemical reactions. The CpTPyP films grown on the ⟨100⟩ surface of Si wafers were pressed against a ZnSe hemispherical crystal with a miniature pressure device to assure optical contact. Repeatedly pressing the coated Si wafer to the ZnSe hemisphere crystal results in identical infrared spectra for both p- and s-polarized geometries; therefore, the monolayer is apparently not damaged or aligned by pressing it against the ZnSe crystal. Figure 2 shows the FTIR-ATR spectra obtained with a single reflection from the interface of the ZnSe crystal and Si/porphyrin monolayer. For both p- and s-polarized incident radiation, two phenyl ring vibrations in the Cp layer were observed at 1605 and 1396 cm^{-1}, which were assigned to $\nu_{16} + \nu_5$ and ν_8 in resonance with $\nu_1 + \nu_6$ on the basis of the original benzene symmetry of E_{1u} and E_{2g}, respectively (Figure 2).[15] After the porphyrin layer (TPyP) was introduced, two strong vibrations were observed at 1635 and 1593 cm^{-1} that are associated with two weak vibrations at 1716 and 1407 cm^{-1} for both incident polarizations. The band at 1716 cm^{-1} is associated with the vibration of C_α–C_m of the porphyrin skeleton.[16] In the s-polarized geometry, an additional vibration at 1450 cm^{-1} arising from a combination of $\nu(C_\beta\text{–}N)$ and $\delta(CCN)$[17] and attributed to the porphyrin ring was also observed. The two strong characteristic bands at 1635 and 1593 cm^{-1} were assigned to ν_{8a} of the N-substituted pyridinium (a_1) and ν_4 modes of the pyridyl groups,[18] respectively, and the simultaneous appearance of these two bands is the signature of an asymmetric structure, i.e., free pyridyl at the outer surface and the pyridinium linkage of the porphyrin to the coupling layer. Therefore the porphyrin monolayer is polar. The intensities of these vibrations of the aromatic rings in the p-polarized geometry are in the region of a few milliabsorbance units (mABS) that corresponds to the thickness of a typical monolayer thin film ($\sim$20 Å).[19]

The intensity of the pyridyl mode at 1593 cm^{-1} can be used

(12) Porphyrin monolayer absorbance at $\lambda_{max} = 447$ nm: 0.0295. Model compound 5,10,15,20-tetrakis(1-methyl-4-pyridyl)-21*H*,23*H*-porphine (tetra-p-tosylate salt): $\lambda_{max}(H_2O) = 422$ nm ($1.5 \times 10^5\ cm^{-1}\ M^{-1}$).

(13) (a) Fleischer, E. B.; Stone, A. L. *Chem. Commun.* **1967**, 332–3. (b) Fleischer, E. B.; Shachter, A. M. *Inorg. Chem.* **1991**, *30*, 3763–9.

(14) (a) Levine, B. F. *Chem. Phys. Lett.* **1976**, *37* (3), 516–520. (b) Oudar, J. L.; Chemla, D. S. *J. Chem. Phys.* **1977**, *66* (6), 2664–2668.

(15) (a) Mair, R. D.; Hornig, D. F. *J. Chem. Phys.* **1949**, *17* (12), 1236–47. (b) Thakur, S. N.; Goodman, L.; Ozkabak, A. G. *J. Chem. Phys.* **1986**, *84* (12), 6642–56. (c) Richardson, N. V. *Surf. Sci.* **1979**, *87*, 662–8. (d) Busca, G.; Zerlia, T.; Lorenzelli, V.; Girelli, A. *J. Catal.* **1984**, *88*, 131–6. (e) Koel, B. E.; Crowell, J. E.; Mate, C. M.; Somorjai, G. A. *J. Phys. Chem.* **1984**, *88*, 1988–6.

(16) C_α, C_β, and C_m stand for alpha, beta, and *meso* carbon atoms.

(17) (a) Ogoshi, H.; Saito, Y.; Nakamoto, K. *J. Chem. Phys.* **1972**, *57* (10), 4194–4202. (b) Sunder, S.; Bernstein, H. J. *J. Raman Spectrosc.* **1976**, *5*, 351–371. (c) Alben, J. O. *The Porphyrins*; Academic Press, Inc.: New York, 1978; Vol. III, pp 323–345.

(18) (a) Bunding, K. A.; Bell, M. I.; Durst, R. A. *Chem. Phys. Lett.* **1982**, *89* (1), 54–58. (b) Kobayashi, Y.; Itoh, K. *J. Phys. Chem.* **1985**, *89*, 5174–5178. (c) Long, D. A.; George, W. O. *Spectrochim. Acta* **1963**, *19*, 1777–1790. (d) Spinner, E. *Aust. J. Chem.* **1967**, *20*, 1805–13.

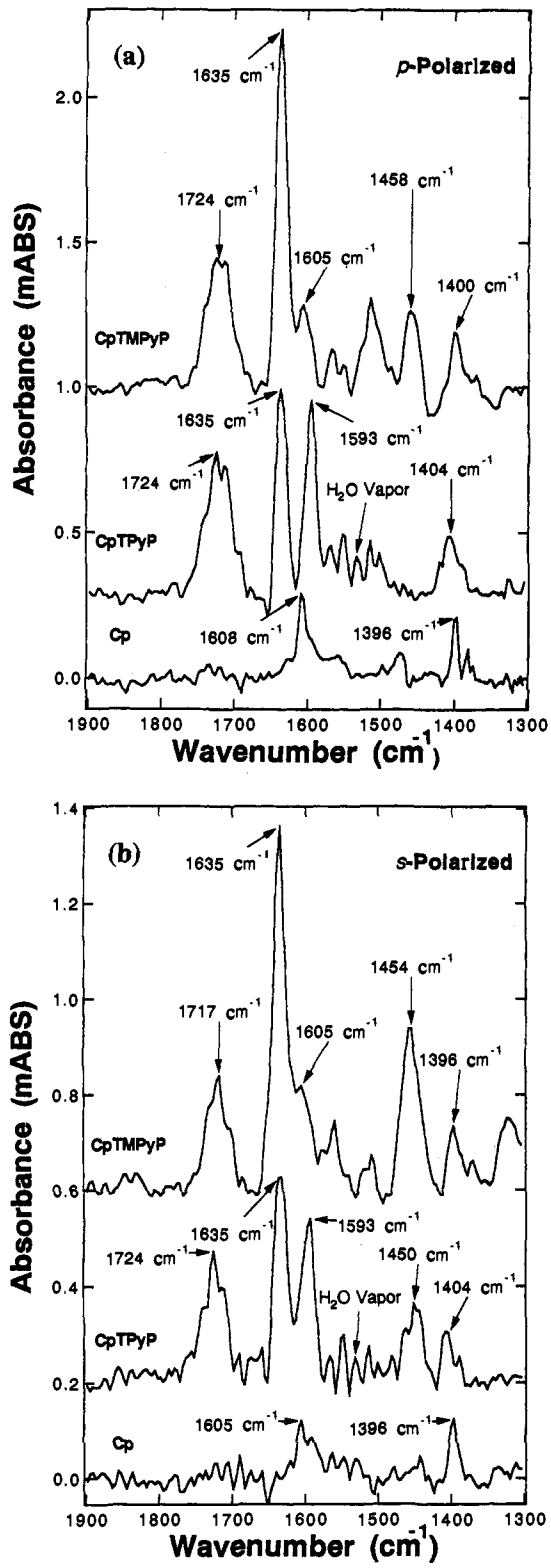

Figure 2. FTIR-ATR spectra of the (p-(chloromethyl)phenyl)trichlorosilane-based coupling layer (Cp) (bottom), the porphyrin layer (CpTPyP) (middle), and the quaternized porphyrin layer (CpTMPyP) (top) covalently bound to the native oxide on Si(100) for (a) p- and (b) s-polarized light incident at 39°: 1024 scans, 8-cm^{-1} resolution. The baseline was corrected to zero absorbance and offset for display purposes.

to diagnose the quaternization of the outer pyridyl groups. For instance, after reacting the porphyrin monolayer with iodomethane, the strong band at 1593 cm^{-1} that corresponds to the ν_4 mode of the pyridyl groups disappeared completely. Conversely, the N-substituted pyridinium ν_{8a} mode increased in intensity because of the conversion of pyridyl groups into pyridinium moieties (Figure 2). The disappearance of the pyridyl mode suggests that the quaternization reaction was complete. Furthermore, the complete disappearance of the pyridyl mode allows the observation of the phenyl mode at 1605 cm^{-1} arising from the coupling layer. The phenyl ring stretching mode from the coupling layer at 1407 cm^{-1} is shifted to 1395 cm^{-1}. The vibration at 1716 cm^{-1} is unchanged throughout the reaction with iodomethane in both p- and s-polarized spectra. The band observed at 1450 cm^{-1} in the s-polarization is enhanced by the quaternization reaction of the available pyridyl moieties.

Nonlinear Optical (NLO) Properties. The nonlinear optical properties of the monolayer film were investigated using second-harmonic generation (SHG) in a transmission geometry. The SHG measurements were made under nonresonant conditions using p- or s-polarized 1064-nm incident radiation from a Nd:YAG regenerative amplifier laser with a ~100-ps pulse width and energy densities at the thin-film surface of 250–500 μJ/mm^2. The transmitted, p-polarized SHG signals at 532 nm from a fused quartz substrate with a CpTPyP monolayer film on each surface of the substrate were measured as the substrate was rotated from normal incidence (0°) to grazing incidence (~90°). There was no measurable nonlinear response from the blank substrates under identical excitation conditions for either incident polarization.

Figure 3 presents the transmitted, p-polarized SHG for both the p- and s-polarized fundamentals at 1064 nm. No strong azimuthal orientation dependence was observed within the plane of the self-assemblies in the SHG experiments, a result which was also supported by the lack of anisotropy in the FTIR measurements of the film. These results indicate that the films possess uniaxial symmetry about the surface normal.[4] Only two independent tensor elements of $\chi^{(2)}$ are then nonvanishing, χ_{zzz} and $\chi_{zxx} = \chi_{zyy}$. The two major features in Figure 3 are the interference pattern and the angular dependent envelope.[4,20] The interference fringes of the SH intensity arise from the interaction of the second-harmonic waves from self-assembled films on both sides of the silica substrate. Their complete destructive interference, i.e. the zero minima, indicates that the thin films on both sides of the substrate are essentially identical, possessing the same molecular orientation or polar angle, number density, chemical structure, and thickness when averaged over an area of the fundamental laser beam diameter. The smooth angular dependent envelope and complete destructive interference pattern further suggest that the laser beam is not destroying the self-assembled porphyrin monolayer. This is confirmed by the fact that there is no measurable change in the optical absorption after the SHG measurements.

Both p- or s-polarized excitation can generate p-polarized SHG, and the induced second-order polarizabilities are described in eqs 1 and eq 2. The first subscript refers to the fundamental

$$P_{p,p}^{2\omega} = \chi_{zzz}E_zE_z + \chi_{zyy}E_yE_y \quad (1)$$

$$P_{s,p}^{2\omega} = \chi_{zxx}E_xE_x \quad (2)$$

polarization, and the second subscript refers to the polarization of the second-harmonic light. Under the same experimental conditions, we found that the ratio $(I_{p,p}/I_{s,p})^{1/2} = 1.74$ in the vicinity of maximum SHG response (56° in Figure 3). A value of $\chi_{zzz}/\chi_{zxx} = 2.29$ was then calculated from eqs 1 and 2. The same ratio χ_{zzz}/χ_{zxx} can be obtained also by fitting eq 1 to the experimental data because the angular dependent nonlinear

(19) (a) Laibinis, P. E.; Whitesides, G. M.; Allara, D. L.; Tao, Y. T.; Parikh, A. N.; Nuzzo, R. G. *J. Am. Chem. Soc.* **1991**, *113*, 7152–7167. (b) Nuzzo, R. G.; Fusco, F. A.; Allara, D. L. *J. Am. Chem. Soc.* **1987**, *109*, 2358–2368. (c) Nuzzo, R. G.; Dubois, L. H.; Allara, D. L. *J. Am. Chem. Soc.* **1990**, *112*, 558–569.

(20) Li, D.; Swanson, B. I.; Robinson, J. M.; Hoffbauer, M. A. *SPIE Proc., Nonlinear Opt. III* **1992**, *1626*, 426–30.

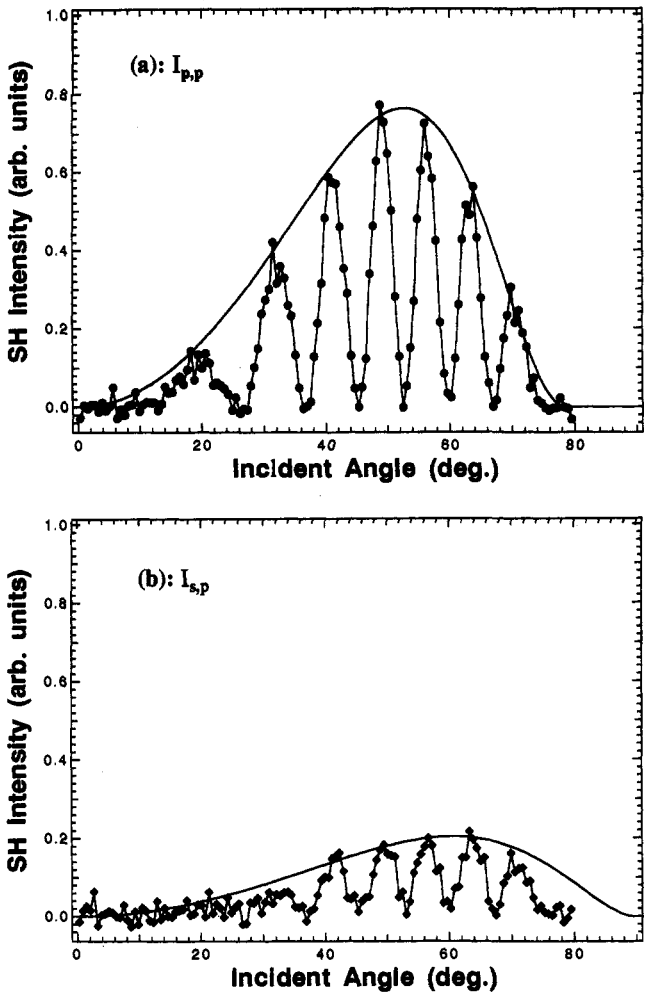

Figure 3. Transmitted p-polarized SH intensity at 532 nm as a function of the angle of the p-polarized (a) and s-polarized (b) incident beam with respect to the surface normal for a fused quartz substrate functionalized with a CpTPyP monolayer on both sides. Each data point represents the average of 100 laser pulses; they are connected by a solid line for visual clarity. The solid lines describing the overall envelopes are theoretical fits to the data as described in the text.

response of $P_{p,p}^{2\omega}$ is governed by this parameter. According to a theoretical model described by Bloembergen[21] and others,[22] the envelope for $I_{p,p}$ (eq 1) is determined by the ratio of the second-order nonlinear susceptibility tensor elements, χ_{zzz}/χ_{zxx}, and by the ratio of the refractive indices, $n_{film}(\omega)/n_{film}(2\omega)$.[23] The solid line in Figure 3a shows a fit to the envelope of the experimental data using the ratios $\chi_{zzz}/\chi_{zxx} = 2.32$ and $n_{film}(\omega)/n_{film}(2\omega) = 1.5$ in the theoretical model. The dispersion of the refractive index is approximately 1, indicating that the experiments were performed under nonresonant conditions, in agreement with the lack of features in the optical spectra at ω and 2ω. Thus, our reported χ_{zzz} will not be enhanced by resonance absorption effects. The transmitted s-polarized SHG from either p- or s-polarized excitation was vanishingly small under the same experimental conditions. This result is consistent with the chromophore having a uniaxial symmetry along the surface normal. Thus, we have employed two independent methods to determine the ratio χ_{zzz}/χ_{zxx}, and the agreement between these two approaches is excellent.

Using a theoretical molecular thickness of 23.4 Å from averaged crystallographic porphyrin bond lengths and bond angles[24] for the chromophore layer, standard bond distances[25] for the coupling layer, and an average polar angle of $\langle\psi\rangle$ of ~43° (*vide infra*), a monolayer CpTPyP film thickness of ~17 Å was calculated. By calibrating the observed SHG intensity to that measured for an uncoated *y*-cut quartz flat[26] at the first Maker fringe, a value of $\chi_{zzz} \sim 2 \times 10^{-8}$ esu was obtained for the monolayer CpTPyP film under the nonresonant conditions used in the present study. The observation of a relatively large SH response from the acentric porphyrin macrocycle monolayer films is consistent with having highly delocalized π-electrons in the porphyrin derivatives.

This value for χ_{zzz} is about 1 order of magnitude smaller than that for a self-assembled monolayer thin film of 4-[*N*,*N*-bis(3-hydroxypropyl)amino]styryl-4′-pyridine ($\chi_{zzz} = 6 \times 10^{-7}$ esu)[4a-c] and smaller than the nonlinear coefficients reported for a monolayer of the polar dye 4-{4-[*N*,*N*-bis(2-hydroxyethyl)-amino]phenylazo}phenylphosphonic acid[4d] ($d_{zxx} = 2.1 \times 10^{-7}$ esu). This comparison indicates that intramolecular charge transfer can affect $\chi_{zzz}^{(2)}$ by about 10-fold in typical organic films. By incorporating charge-transfer functionalities in the present system, the magnitude of $\chi_{zzz}^{(2)}$ could likely be increased.

Orientation of Surface-Bound Porphyrin Monolayer. The experimentally determined ratio χ_{zzz}/χ_{zxx} can be used to calculate the average molecular orientation, $\langle\psi\rangle$, defined as the angle of the dipole moment of the chromophore with respect to the surface normal.[27] For aromatic molecules with delocalized electrons, the molecular tensor along the dipole direction, $\beta_{\zeta\zeta\zeta}$, typically predominates.[28] The in-plane molecular transition dipole moments are often larger than those perpendicular to the molecular plane, and transition moments along the transition dipole are larger than those perpendicular to it. Assuming that $\beta_{\zeta\zeta\zeta}$ is the dominant tensor, eqs 3 and 4 relate the magnitude of the nonvanishing nonlinear susceptibilities of the film to the average molecular orientation $\langle\psi\rangle$,[27] where N is the molecular number density and C is the local field correction factor.

$$\chi_{zzz} = NC\beta_{\zeta\zeta\zeta}\langle\cos^3\psi\rangle \quad (3)$$

$$\chi_{zxx} = \frac{1}{2}NC\beta_{\zeta\zeta\zeta}\langle\sin^2\psi\cos\psi\rangle \quad (4)$$

Covalently bound self-assemblies are typically highly ordered,[29] and therefore, it is generally a good approximation to assume that the molecular orientation angle, ψ, has a narrow distribution near its average mean value, $\langle\psi\rangle$. Using this approximation, eqs 3 and 4 can be simplified as $\chi_{zzz}/\chi_{zxx} = 2\langle\cot^2\psi\rangle = 2\cot^2\langle\psi\rangle = 2.3$. This ratio, $\chi_{zzz}/\psi_{zxx} = 2\cot^2\langle\psi\rangle$, yields the average angle between the molecular dipole moment and the surface normal for these porphyrin self-assembled monolayers of $\langle\psi\rangle = 43 \pm 3°$.

The orientation of the porphyrin overlayer on the surface of the Si wafer can also be determined from the polarized FTIR-

(21) Bloembergen, N.; Pershan, P. S. *Phys. Rev.* **1962**, *128*, 606–22.
(22) (a) Zhang, T.; Zhang, C.; Wong, G. K. *J. Opt. Soc. Am. B* **1990**, *7*, 902–7. (b) Marowsky, G.; Lüpke, G.; Steinhoff, R.; Chi, L. F.; Mobius, D. *Phys. Rev. B* **1990**, *41* (7), 4480–3.
(23) In fitting to the theoretical model, the refractive indices used for air and glass are $n_{air}(\omega) = 1.00$, $n_{glass}(\omega) = 1.50$, and $n_{glass}(2\omega) = 1.55$.
(24) Smith, K. M. *Comprehensive Heterocyclic Chemistry*, Pergamon Press: New York, 1984; p 386.
(25) Lide, D. R. *Handbook of Chemistry and Physics*, 72nd ed.; CRC Press: Boston, 1991; pp 9-2–9-17.
(26) Maker, P. D.; Terhune, R. W.; Nisenoff, M.; Savage, C. M. *Phys. Rev. Lett.* **1962**, *8*, 21–2.
(27) (a) Shen, Y. R. In *Chemistry and Structure at Interfaces: New Laser and Optical Techniques*; Hall, R. B., Ellis, A. B., Eds.; VCH Publishers, Inc.: Deerfield Beach, FL, 1986; Chapter 4, p 171. (b) Williams, D. J. *Angew. Chem., Int. Ed. Engl.* **1984**, *23*, 690.
(28) (a) Li, D.; Marks, T. J.; Ratner, M. A. *Chem. Phys. Lett.* **1986**, *131*, 370–375. (b) Li, D.; Marks, T. J.; Ratner, M. A. *J. Am. Chem. Soc.* **1988**, *110*, 1707–1715.
(29) (a) Chen, C. H.; Vesecky, S. M.; Gewirth, A. A. *J. Am. Chem. Soc.* **1992**, *114*, 451–458. (b) Weisenhorn, A. L.; Egger, M.; Ohnesorge, F.; Gould, S. A. C.; Heyn, S. P.; Hansma, H. G.; Sinsheimer, R. L.; Gaub, H. E.; Hansma, P. K. *Langmuir* **1991**, *7*, 8–12. (c) Kim, Y. T.; Bard, A. J. *Langmuir* **1992**, *8*, 1096–1102. (d) Tsao, Y. H.; Yang, S. X.; Evans, D. F. *Langmuir* **1992**, *8*, 1188–1194. (e) Chidsey, C. E. D.; Liu, G. Y.; Scoles, G.; Wang, J. *Langmuir* **1990**, *6*, 1804–1806. (f) Samant, M. G.; Brown, C. A.; Gordon, J. G., II. *Langmuir* **1991**, *7*, 437–439. (g) Walczak, M. M.; Chung, C.; Stole, S. M.; Widrig, C. A.; Porter, M. D. *J. Am. Chem. Soc.* **1991**, *113*, 2370–2378. (h) Widrig, C. A.; Alves, C. A.; Porter, M. D. *J. Am. Chem. Soc.* **1991**, *113*, 2805–2810.

ATR measurements. By using a theoretical model described by Milosevic,[30] oscillator strength parallel ($f_\parallel$) and perpendicular ($f_\perp$) to the surface can be obtained by fitting the experimental data to the calculated spectra. This model treated the sample as a self-assembled layer covalently bound to the native oxide of the Si wafer and accounted for all three individual layers in the internal reflection technique, i.e., the film CpTPyP layer (n_{film}), the native oxide layer (n_{quartz}), and the Si substrate (n_{Si}). The refractive indices used in the fitting are $n_{film} = 1.5$, $n_{quartz} = 1.45$, and $n_{Si} = 3.45$. The infrared intensity of the pyridyl mode is not sensitive to the change in the thickness of the Si substrate and the native oxide (SiO_2) layer over a few orders of magnitude. Considering the mode of the pyridyl group at 1593 cm^{-1}, the absorption intensities of p-polarized and s-polarized spectra are $I_p = 0.74$ mABS and $I_s = 0.43$ mABS, respectively. By fitting the experimental absorbances at 1593 cm^{-1} according to the theoretical model, the oscillator strength (f) of this particular mode under both p- and s-polarized geometries was obtained. The ratio of the oscillator strength parallel and perpendicular to the surface, $f_\parallel/f_\perp = 0.87$, can be related to the orientation of this particular mode as $f_\parallel/f_\perp = \langle \tan^2\theta \rangle$,[31] where θ is the angle between the surface normal and the dipole moment of this particular mode. Assuming a narrow distribution for the molecular orientation angle, an average alignment angle, $\langle\theta\rangle$, of 43° is obtained for this mode, that is in excellent agreement with the polar angle, $\langle\psi\rangle$, measured using surface second-harmonic generation.

(30) Milosevic, M.; Berets, S. L. Paper submitted to *Appl. Spectrosc.*

(31) (a) Harrick, N. J.; Mirabella, F. M. *Internal Reflection Spectroscopy: Review and Supplement*; Harrick Scientific Corp.: New York, 1985. (b) Painter, P. C.; Coleman, M. M.; Koenig, J. L. *The Theory of Vibrational Spectroscopy and Its Application to Polymeric Materials*; Wiley & Sons: New York, 1982. (c) Allara, D. L.; Nuzzo, R. G. *Langmuir* **1985**, *1*, 52–66. (d) Porter, M. D.; Bright, T. B.; Allara, D. L.; Chidsey, C. E. D. *J. Am. Chem. Soc.* **1987**, *109*, 3559–3568.

Conclusions

The results presented in this paper show that both FTIR-ATR and SHG are very useful techniques for the characterization of self-assembled monolayer thin-film systems. These techniques reveal that the porphyrin monolayer is highly ordered and closely packed in its solid-state structure. The observation of a relatively large SHG response ($\chi_{zzz} \sim 2 \times 10^{-8}$ esu) from the acentric covalently bonded, self-assembled macrocycle monolayer films can be attributed to the completely delocalized π-electrons in the porphyrin derivatives. The average molecular orientation of the porphyrin monolayer relative to the surface normal of the substrates (Si and SiO_2) has also been experimentally determined.

Acknowledgment. This work was performed under the auspices of the Department of Energy. The authors acknowledge the support of the Center for Material Science at LANL, the DOE Basic Energy Sciences, and Laboratory Directed Research and Development. D.L. was supported by a LANL Director's Funded Postdoctoral Fellowship. We thank J.D. Farr for performing the XPS measurements.